2014

On tropical cyclone size and intensity changes associated with two types of long-lasting rainbands in monsoonal environments

Chen, Buo-Fu

AGU PUBLICATIONS

Geophysical Research Letters

RESEARCH LETTER
10.1002/2014GL059368

Key Points:
- TC size and intensity changes documented
- OMCS does not change size
- ERB changes size and intensity

Correspondence to:
R. L. Elsberry,
Elsberry@nps.edu

Citation:
Chen, B.-F., C.-S. Lee, and R. L. Elsberry (2014), On tropical cyclone size and intensity changes associated with two types of long-lasting rainbands in monsoonal environments, *Geophys. Res. Lett.*, *41*, 2575–2581, doi:10.1002/2014GL059368.

Received 21 JAN 2014
Accepted 12 MAR 2014
Accepted article online 17 MAR 2014
Published online 1 APR 2014

On tropical cyclone size and intensity changes associated with two types of long-lasting rainbands in monsoonal environments

Buo-Fu Chen[1], Cheng-Shang Lee[1,2], and Russell L. Elsberry[3]

[1]Department of Atmospheric Sciences, National Taiwan University, Taipei, Taiwan, [2]Taiwan Typhoon and Flood Research Institute, National Applied Research Laboratories, Taipei, Taiwan, [3]Department of Meteorology, Naval Postgraduate School, Monterey, California, USA

Abstract Tropical cyclones (TCs) in a monsoonal environment may have heavy rain events separate from the eyewall rainfall. Two types of long-lasting rainbands in western North Pacific TCs interacting with the East Asia summer monsoon during 1999–2009 are identified and the effects of these rainbands on TC size and intensity changes are examined. For all of the south-type Outer Mesoscale Convective Systems as defined in our previous study, the TC intensification rate is decreased but the rate of size change is not modified. Long-lasting south-type Enhanced Rainbands (ERBs) that develop between 100 and 300 km radii and move cyclonically are associated with significant TC size increases. Seventy percent of very large typhoons had an ERB during the period when they intensified from tropical storms to typhoons.

1. Introduction

Intensity (maximum sustained winds), strength (average wind in 100–200 km radial band), and size (radius of 34 kt winds) are three properties that have been defined by *Holland and Merrill* [1984] to describe the tropical cyclone (TC) wind structure. Intensity is critically important because the wind-related damage is proportional to at least the square of the maximum surface winds. However, the outer vortex wind profile (related to strength and size) is also important for TC forecasts and warnings of wind damage [*Powell and Reinhold*, 2007], storm surge [*Irish et al.*, 2008], surface wave heights [*Sampson et al.*, 2013], and timing of the arrival of gale-force winds [*Stenger and Elsberry*, 2013]. Early observational studies documented that the dynamical processes leading to size changes often differ from those involved in intensity changes [*Merrill*, 1984; *Weatherford and Gray*, 1988; *Cocks and Gray*, 2002]. However, a recent study by *Chan and Chan* [2012] has shown that size is strongly correlated ($\Gamma = 0.9$) to outer core strength. The focus of this study is on both the intensity and the size changes during and following the occurrence of two types of long-lasting rainbands in western North Pacific TCs that are interacting with the summer monsoon.

Generally, the TC outer wind structure varies due to interactions with different environmental flows. For western North Pacific TCs, strong low-level southwesterly summer monsoon or northeasterly monsoonal flows in the autumn are favorable for the development of large TCs [*Liu and Chan*, 1999; *Lee et al.*, 2010]. Vertical shear of the horizontal wind (VWS) may have an important role in TC developments and structure via inducing asymmetric convective features [*Frank and Ritchie*, 1999], venting moisture and energy out of the TC core [*Tang and Emanuel*, 2012], and transporting low-entropy air into the inflow boundary layer [*Riemer et al.*, 2010].

Development of TC rainbands owing to various TC/environment interactions may also lead to structural changes. A numerical simulation by *Wang* [2009] indicated that the heating in rainbands may increase TC size but decrease the TC intensity. Furthermore, the rainband activity is an important factor in the formation of annular hurricanes [*Knaff et al.*, 2003, 2008], concentric eyewalls [*Wang*, 2009], and compact typhoons [*Chen et al.*, 2011, 2012].

Various physical mechanisms for the effect of rainbands on TC intensity have been proposed. First, the low-level convergence and ascent in the rainbands may block the boundary layer inflow and thus reduce the convection near the eyewall and negatively affect TC intensification [*Willoughby et al.*, 1982; *Shapiro and Willoughby*, 1982]. Second, air with low equivalent potential temperature (θ_e) injected into the inflow boundary layer by convective-scale downdrafts as the rainband develops also has negative impacts on TC intensification [*Barnes et al.*, 1983; *Powell*, 1990]. *Riemer et al.* [2010] further indicate that this rainband (convection asymmetry)

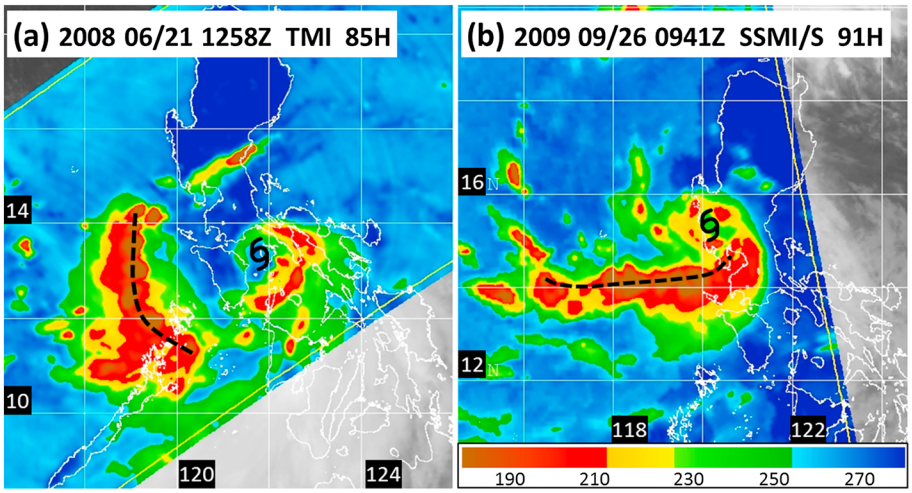

Figure 1. Satellite passive microwave brightness temperature observations for (a) the OMCS that occurred in the outer circulation of Typhoon Fengshen at around 1300 UTC 21 June 2008 and (b) the ERB that occurred within the circulation of Typhoon Katsana at around 1000 UTC 26 September 2009. The black-dotted lines indicate the convective bands of the OMCS and ERB. These figures are adapted from the Naval Research Laboratory website (www.nrlmry.navy.mil/tc_pages/tc_home.html).

may be associated with VWS. Furthermore, rainbands may promote TC intensity changes when the cyclonic potential vorticity (PV) generated in the midtroposphere stratiform precipitation region constitutes an important PV source for inner-core spin-up [*May and Holland*, 1999; *Hill and Lackmann*, 2009].

The first type of long-lasting rainbands that are associated with the TC/monsoon interaction [*Chien and Kuo*, 2011; *Lee et al.*, 2011] is an Outer Mesoscale Convective System (OMCS, Figure 1a), which is a long-lived and cold-topped linear convective system that has a thick and large stratiform precipitation region in the outer region of a TC [*Lee et al.*, 2012]. The second type, which is termed as an Enhanced Rainband (ERB, Figure 1b), is identified in this study as a transformation of the TC principal rainband to have a larger cold cloud shield and longer duration due to an interaction with the monsoon environment. It is emphasized that some of these long-lasting convective events that are separate from the central core of deep convection are also an important forecast and warning problem because they lead to "unexpected heavy rain events" [*Lee et al.*, 2012].

Methodology to identify OMCSs and ERBs and their climatological characteristics are presented in section 2. The TC size and intensity changes associated with the occurrences of OMCSs and ERBs based on Joint Typhoon Warning Center (JTWC) best tracks are summarized in section 3. A tendency for the ERB events to be associated with the larger TCs will be described in section 4. Summary and discussion are provided in section 5.

2. Outer Mesoscale Convective Systems and Enhanced Rainbands

Lee et al. [2012] identified the 109 OMCSs in the western North Pacific from 1999 to 2009 by using a two-step procedure that first examined an hourly infrared channel-1 cloud top temperature data set (IR1) and second utilized passive microwave images (PMW). The advantage of this IR1 data set is the continuous, high-frequency infrared imagery [*Maddox*, 1980; *Williams and Houze*, 1987] for tracking long-lived convective systems associated with TCs every hour. Lee et al. first identified 603 long-lasting ($>$ 6 h) convective systems with a contiguous cold cloud shield (CCS) with IR1 brightness temperatures less than -65°C that exceeded 72,000 km^2 in area. In the second step, *Lee et al.* [2012] utilized PMW imagery to identify 109 OMCSs among these 603 long-lasting CCSs with -55°C PMW brightness temperature (color yellow in Figure 1) that were required to be at least 200 km from the inner-core convection. In addition, the radial extent of the band axis (black-dotted line in Figure 1a) should be shorter than the azimuthal extent.

In this study, a separate set of 90 of these 603 long-lasting CCSs has been classified as ERBs based on the following criteria: (i) The downwind end of the rainband should be connected to the inner core; (ii) the convective axis of the ERBs should have an longer radial extent than azimuthal extent (black-dotted line in Figure 1b); and (iii) the center point of ERB must be at least 100 km from the TC center. These criteria distinguish ERBs from the other 404 long-lasting CCSs that are associated with the eyewall or asymmetric

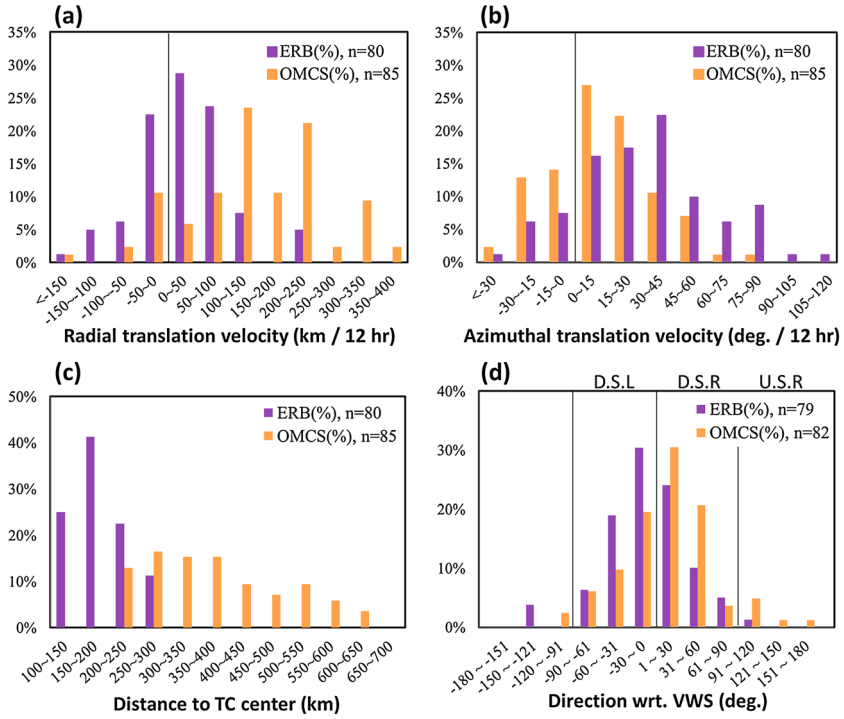

Figure 2. Histograms of the percentages of south-type OMCSs and south-type ERBs for (a) radial translation speeds, (b) azimuthal translation speeds, (c) distances from OMCS (ERB) centers to the TC centers, and (d) orientations with respect to the VWS vectors, where D.S.L., D.S.R., and U.S.R. stand for downshear left, downshear right, and upshear right.

convection near the TC center. The mean durations of 10.3 h for these OMCSs and 12.2 h for these ERBs are sufficient to characterize them as long-lasting rainband systems that may have considerable societal impacts.

In this study, the focus is on 85 "south-type" OMCSs and 80 ERBs that occur in the southern semicircle of the TC circulation as it interacts with the monsoonal flow. Among these south-type OMCSs and ERBs, 82% of the OMCSs and 75% of the ERBs occurred during June–September and also frequently developed to the west of 140°E. Another characteristic of the ERBs is that they occurred most frequently during the tropical storm stage. In general, these south-type ERBs and OMCSs develop in similar synoptic conditions (e.g., strong low-level southwesterly flows, strong northeasterly deep-layer mean VWS, and a moist, low-level monsoon environment).

Whereas OMCSs developed in distant rainbands between 200 km and 700 km from the TC center (Figure 2c), and had a predominant outward propagation (Figures 2a and 2b), ERBs developed from the primary rainband between 100 km and 300 km radius (Figure 2c) and had a predominant cyclonic propagation (Figure 2b). Consistent with the previous studies of *Corbosiero and Molinari* [2003] and *Riemer et al.* [2010], asymmetric convection was favored in the downshear-right quadrant for the OMCS in the outer rainband region and in the downshear-left quadrant for the ERB in the inner-core region with respect to 850–200 hPa deep-layer mean (in a radial ring of 200–800 km from the center) VWS (Figure 2d). Since these orientations of the shear vectors are related to the low-level westerly monsoonal flow, the VWS orientation may be one of the important factors determining the development and azimuthal variations of these long-lasting rainbands.

3. Effects of Long-Lasting Rainbands on Normalized TC Intensity and Size

Although both the south-type OMCSs and ERBs generally occur in conjunction with the summer monsoon environment, their different distances and motions relative to the TC center are hypothesized to be related to the heating source around the TC vortex and the interaction between the heating-generated PV and the vortex circulation. Thus, different TC size and intensity evolutions are also expected related to the occurrences of OMCSs and ERBs.

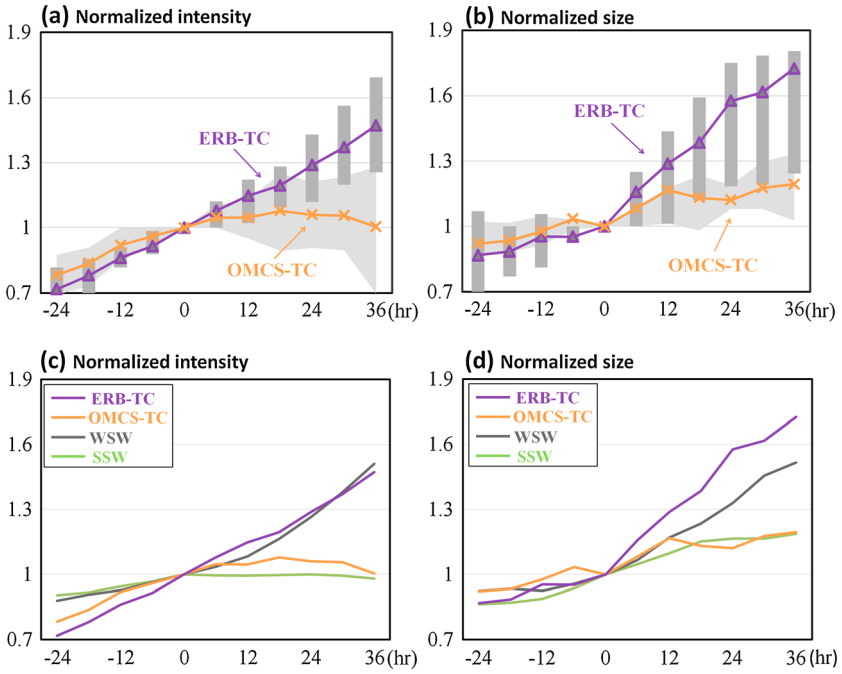

Figure 3. Time series of the average, upper quartile (75%) and lower quartile (25%) of the (a) normalized intensity and (b) normalized size for TC-groups OMCS-TC and ERB-TC, where the time "0" indicates the initiation times of the OMCSs and ERBs. Time series of the (c) mean normalized intensity and the (d) mean normalized size for TC-groups OMCS-TC and ERB-TC, and for the weak southwesterly (WSW) and strong southwesterly (SSW) monsoon flow samples with a reference time 0 (see inset for line color definitions).

Normalized intensity and normalized size changes relative to the values at the initiation time of the associated OMCS/ERB are calculated based on Joint Typhoon Warning Center (JTWC) best-track files for TCs during 2002–2009, as JTWC only began providing the radii of the 35 kt winds after August 2001. The average of the radii of 35 kt winds in the four quadrants is defined as the TC size.

In this TC sample, the OMCS-TC or ERB-TC had to be at least 200 km from land from 24 h before initiation to 24 h after termination and of at least tropical storm intensity ($>$ 35 kt) during this period. The evolutions of the average, upper quartile (75%) and lower quartile (25%) of normalized intensity and normalized size for the TCs producing OMCSs (OMCS-TC, 18 cases) or ERBs (ERB-TC, 22 cases) are displayed in Figures 3a and 3b. Note that the normalized intensity and size changes of the ERB-TC were similar to those of the OMCS-TC before the initiation time. After the ERBs occurred, the TC size (Figure 3b) increased at a faster rate than occurred after the OMCSs. After the OMCSs (ERBs) occurred, the intensification rate (Figure 3a) decreased (remained almost constant).

To explore the most-likely environmental impact of VWS, the intensity and size evolutions are examined for a second sample of 29 TCs that encountered strong southwesterly monsoon flows (labeled SSW) and 29 TCs that encountered weak southwesterly flows (labeled WSW) but produced no OMCSs or ERBs. The strength of southwesterly flows is defined as the average wind speed at 850 hPa in the area 400 km south to 1200 km south and 1200 km east to 800 km west of the TC center. These cases occurred from June to September and met the following criteria: (i) TC is south of 26°N and west of 145°E, (ii) TC is 200 km from land from 24 h before to 36 h after the reference time, and (iii) similar distributions of TC intensity existed for these two subsamples as for the TCs that did have an OMCS or an ERB.

The larger TC intensities for WSW monsoon flow than for the SSW (Figure 3c) are expected because the VWS of the SSW monsoon flow is much larger than for the WSW. Although the magnitudes of southwesterly flows associated with OMCS-TC, ERB-TC, and SSW at the $t = 0$ reference times were comparable (10.6 m s^{-1}, 11.9 m s^{-1}, and 11.9 m s^{-1}, respectively), the TC intensification rate of an ERB-TC is quite similar to that of the WSW monsoon flow (Figure 3c). By contrast, the occurrence of an OMCS-TC led to a marked decrease in the rate of intensification that then became comparable to the TCs in a SSW monsoon flow.

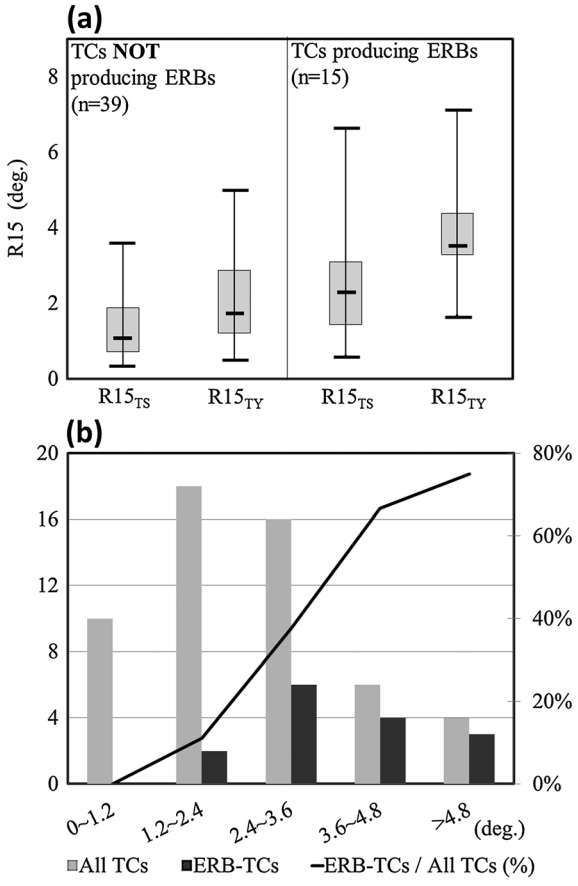

Figure 4. (a) Box-and-whisker chart of the radii of 15 m s^{-1} winds (R15) of TCs intensifying from 30–40 kt (labeled R15TS) to 60–70 kt (labeled R15TY) while producing no ERBs (39 cases) or producing ERBs (15 cases) during their TS stage. (b) Histogram of the R15TY sizes (degrees latitude) among the 54 TCs in the ALL TCs sample (grey bars, left ordinate) and among the 15 TCs producing ERBs (black bars, left ordinate). The thick black line indicates the ratio (percent, right ordinate) of ERB-TCs to All TCs.

As noted in section 1, *Liu and Chan* [1999] and *Lee et al.* [2010] found a strong southwesterly monsoon flow is favorable for the development of large TCs in summer. The TC size increase after the occurrence of the ERB-TC is even larger than for the WSW monsoon flow, with an average 70% increase in normalized size (Figure 3d). Since the normalized intensities of the ERB-TC and WSW at $t + 36$ h in Figure 3c were essentially the same, and assuming the modified Rankine vortex vr^x = constant applies to the radius of 35 kt winds, the larger size for the ERB-TC in Figure 3d may indicate either a larger radius of maximum winds or a flatter outer wind profile (smaller exponent x) for ERB-TC. Note that the OMCS-TC has the same TC size tendency as for the SSW monsoon flow (Figure 3d), just as it has the same TC intensity tendency (Figure 3c). Thus, it is the occurrence of the inner-region rainband ERB that has the larger and more consistent wind structure impact in terms of an increase in size. However, a continuous increase in intensity for the ERB cases in this study tends to conflict with the *Willoughby et al.* [1982], *Shapiro and Willoughby* [1982], *Barnes et al.* [1983], and *Powell* [1990] studies that found an intensity decrease. Even in the numerical simulation by *Wang* [2009] that resulted in a size increase, the TC intensity was also decreased rather than increased as in the ERB cases.

4. ERBs Produced in Tropical Storm Stage may Favor Large-Size Typhoons

The dependency on the actual size of the TC is examined in this section based on Quick Scatterometer data. Using the same methodology as *Lee et al.* [2010], the radii of 15 m s^{-1} speeds of wind (R15) are estimated for the 54 TCs that intensified to at least typhoon intensity during 2000–2009. These 54 TCs are classified into two groups: R15 sizes for 15 TCs that produced a south-type ERB while intensifying from 30–40 kt (labeled as TS) to 60–70 kt (labeled as TY) and for 39 TCs that did not produce an ERB.

The box-and-whisker charts of the $R15_{TS}$ and $R15_{TY}$ for these two groups are displayed in Figure 4a. Note that the TCs producing ERBs typically have consistently larger median and upper and lower quartile sizes at the TS stage than for the No-ERB sample. Thus, occurrence of an ERB may be favored for larger TSs. Furthermore, the R15 size increase from the TS stage to the TY stage is much larger (~ 1.2°) for those TCs that have an ERB than the R15 size increase (~ 0.6°) for the TCs that did not produce an ERB. Therefore, the occurrence of an ERB may promote the occurrence of a large TC.

The tendency for ERBs to occur with larger typhoons relative to the size ($R15_{TY}$) distribution of the ALL sample of TCs without an ERB is confirmed in Figure 4b. That is, 63% of the large TCs with $R15_{TY}$ greater than 3.2° (67% percentile of the 54 cases in the ALL TCs sample) and 70% of very large TCs with $R15_{TY}$ greater than 3.6° had an ERB during the period when they intensified from TS stage to TY stage. Among the 54 TCs in the ALL sample, only six TCs had a south-type OMCS when they intensified from TS to TY. However, five of these TCs that had an OMCS also had an ERB as well, and four of the five developed into very large TCs.

In summary, the statistics in Figure 4 indicate a tendency for larger TSs to have an ERB, and that those TSs are more likely to have larger R15 sizes at the TY stage, which is consistent with the larger normalized intensity and normalized sizes in Figure 3 for the ERB occurrences. Further investigations of the physical responses of these long-lasting rainbands associated with TCs interacting with the southwesterly monsoon flow are necessary for understanding the evolution of TC size and the structure.

5. Summary and Discussion

From 1999 to 2009, 80 south-type ERBs and 85 south-type OMCSs that were associated with TCs influenced by southwesterly monsoon flows have been analyzed to understand their correlations on TC intensity and size. Whereas OMCSs usually developed from distant rainbands between 200 km and 700 km from the TC center, ERBs usually developed from the primary rainband between 100 km and 300 km radius. The VWS orientation may be one of the important factors determining the azimuthal variations of these long-lasting rainbands that OMCS (ERB) was favored in the downshear-right (downshear-left) quadrant. Furthermore, the OMCSs typically propagated more outward with respect to the TC center, and the ERBs usually moved more cyclonically. The primary conclusion is that the occurrence of a long-lasting ERB coincides with an increase in TC size and maintenance in TC intensification (rather than previous suggestions for an intensity decrease). These ERBs are more likely to occur in larger tropical storms (TSs) and tend to lead to larger typhoon (TY) sizes than in a sample of typhoons that did not have an ERB during the intensification from TS to TY. By contrast, the long-lasting OMCSs did not lead to significantly larger TC sizes and tended to be associated with a reduced TC intensification rate.

The basic hypothesis was that ERBs and OMCSs would affect TC size and intensity differently due to the heating effects and the heating-generated PV interactions with the TC vortex. *May and Holland* [1999] and *Hill and Lackmann* [2009] suggested the cyclonic PV generated in the mid-troposphere stratiform precipitation region of the outer rainband (here an ERB) may be wrapped into the inner core and thus become an important PV source to result in both size expansion and intensification. *Didlake and Houze* [2013] documented the dynamical structure of the stratiform sector in the downwind portion of a TC stationary rainband complex. Whereas rising radial outflow occurs within the stratiform cloud layer, downward transport occurs in the descending radial inflow in response to latent cooling beneath the melting level. They further show that this stratiform-induced secondary circulation results in convergence of angular momentum above the boundary layer and broadening of the storm's rotational wind field. Therefore, the dynamical structure of the downwind portion of ERBs may have a role in the midlevel PV being able to reach the inner core.

Understanding the physical mechanisms that determine whether and how an OMCS or an ERB occurrence in a TC interacting with the southwesterly monsoon flow will hopefully lead to improved TC size and intensity forecasts, as well as forecasts of heavy rain areas separate from the TC center. Numerical experiments of the interactions of TCs with various initial vortex structures and various idealized monsoonal environments are proposed to understand the conditions leading to an ERB or OMCS occurrence. These simulations will also be useful to examine the roles of VWS and the moisture distribution in the formation of OMCSs and ERBs, and then to how these long-lasting rainbands lead to TC structure changes documented in this study.

Acknowledgments

Buo-Fu Chen is supported by the National Taiwan University, and Professor Cheng-Shang Lee is supported by the National Taiwan University and the Taiwan Typhoon Flood Research Institute, of the National Applied Research Laboratories. This research is supported by the National Science Council of the Republic of China (Taiwan) under grants of NSC 102-2917-I-002-107 and NSC 99-2625-M-002-013-MY3. Russell L. Elsberry is supported by the Marine Meteorology section, Office of Naval Research. Penny Jones provided excellent assistance in the manuscript preparation.

The Editor thanks two anonymous reviewers for their assistance in evaluating this paper.

References

Barnes, G. M., E. J. Zipser, D. P. Jorgensen, and F. D. Marks Jr. (1983), Mesoscale and convective structure of a hurricane rainband, *J. Atmos. Sci.*, *40*, 2125–2137.

Chan, K. T. F., and J. C. L. Chan (2012), Size and strength of tropical cyclones as inferred from QuikSCAT data, *Mon. Weather Rev.*, *140*, 811–824.

Chen, D. Y., K. K. W. Cheung, and C. S. Lee (2011), Some implications of core regime wind structures in western North Pacific tropical cyclones, *Weather Forecasting*, *26*, 61–75.

Chen, D. Y., K. K. W. Cheung, and C. S. Lee (2012), A study on the synoptic-dynamical characteristics of compact tropical cyclones in the western North Pacific, *Mon. Weather Rev.*, *140*, 4046–4065.

Chien, F. C., and H. C. Kuo (2011), On the extreme rainfall of Typhoon Morakot (2009), *J. Geophys. Res.*, *116*, D05104, doi:10.1029/2010JD015092.

Cocks, S. B., and W. M. Gray (2002), Variability of the outer wind profiles of western North Pacific typhoons: Classifications and techniques for analysis and forecasting, *Mon. Weather Rev.*, *130*, 1989–2005.

Corbosiero, K. L., and J. Molinari (2003), The relationship between storm motion, vertical wind shear, and convective asymmetries in tropical cyclones, *J. Atmos. Sci.*, *60*, 366–376.

Didlake, A. C., Jr., and R. A. Houze Jr. (2013), Dynamics of the stratiform sector of a tropical cyclone rainband, *J. Atmos. Sci.*, *70*, 1891–1911.

Frank, W. M., and E. A. Ritchie (1999), Effects on environmental flow upon tropical cyclone structure, *Mon. Weather Rev.*, *127*, 2044–2061.

Hill, K. A., and G. M. Lackmann (2009), Influence of environmental humidity on tropical cyclone size, *Mon. Weather Rev.*, *137*, 3294–3315.

Holland, G. J., and R. T. Merrill (1984), On the dynamics of tropical cyclone structural changes, *Q. J. R. Meteorol. Soc.*, *110*, 723–745.

Irish, J. L., D. T. Resio, and J. J. Ratcliff (2008), The influence of storm size on hurricane surge, *J. Phys. Oceanogr.*, *38*, 2003–2013.
Knaff, J. A., J. P. Kossin, and M. DeMaria (2003), Annular hurricanes, *Weather Forecasting*, *18*, 204–223.
Knaff, J. A., T. A. Cram, A. B. Schumacher, J. P. Kossin, and M. DeMaria (2008), Objective identification of annular hurricanes, *Weather Forecasting*, *23*, 17–28.
Lee, C. S., K. K. W. Cheung, W. T. Fang, and R. L. Elsberry (2010), Initial maintenance of tropical cyclone size in the western North Pacific, *Mon. Weather Rev.*, *138*, 3207–3223.
Lee, C. S., C. C. Wu, T. C. C. Wang, and R. L. Elsberry (2011), Advances in understanding the "Perfect monsoon-influenced typhoon": Summary from International Conference on Typhoon Morakot (2009), *Asia Pac. J. Atmos. Sci.*, *47*, 213–222.
Lee, C. S., B.-F. Chen, and R. L. Elsberry (2012), Long-lasting convective systems in the outer region of tropical cyclones in the western North Pacific, *Geophys. Res. Lett.*, *39*, L21812, doi:10.1029/2012GL053685.
Liu, K. S., and J. C. L. Chan (1999), Size of tropical cyclones as inferred from ERS-1 and ERS-2 data, *Mon. Weather Rev.*, *127*, 2992–3001.
Maddox, R. A. (1980), Mesoscale convective complexes, *Bull. Am. Meteorol. Soc.*, *61*, 1374–1387.
May, P. T., and G. J. Holland (1999), The role of potential vorticity generation in tropical cyclone rainbands, *J. Atmos. Sci.*, *56*, 1224–1228.
Merrill, R. T. (1984), A comparison of large and small tropical cyclones, *Mon. Weather Rev.*, *112*, 1408–1418.
Powell, M. D. (1990), Boundary layer structure and dynamics in outer hurricane rainbands, Part II: Downdraft modification and mixed layer recovery, *Mon. Weather Rev.*, *118*, 918–938.
Powell, M. D., and T. A. Reinhold (2007), Tropical cyclone destructive potential by integrated kinetic energy, *Bull. Am. Meteorol. Soc.*, *88*, 513–526.
Riemer, M., M. T. Montgomery, and M. E. Nicholls (2010), A new paradigm for intensity modification of tropical cyclones: Thermodynamic impact of vertical wind shear on the inflow layer, *Atmos. Chem. Phys.*, *10*, 3163–3188.
Sampson, C. R., P. A. Wittman, E. A. Serra, H. T. Tolman, J. Schauer, and T. Marchok (2013), Evaluation of wave forecasts consistent with tropical cyclone warning center wind forecasts, *Weather Forecasting*, *28*, 287–294.
Shapiro, L. J., and H. E. Willoughby (1982), The response of balanced hurricanes to local sources of heat and momentum, *J. Atmos. Sci.*, *39*, 378–394.
Stenger, R. A., and R. L. Elsberry (2013), Outer vortex wind structure changes during and following tropical cyclone secondary eyewall formation, *Trop. Cyclone Res. Rev.*, *2*, 184–195.
Tang, B., and K. Emanuel (2012), A ventilation index for tropical cyclones, *Bull. Am. Meteorol. Soc.*, *93*, 1901–1912.
Wang, Y. (2009), How do outer spiral rainbands affect tropical cyclone structure and intensity?, *J. Atmos. Sci.*, *66*, 1250–1273.
Weatherford, C., and W. M. Gray (1988), Typhoon structure as revealed by aircraft reconnaissance, Part II: Structural variability, *Mon. Weather Rev.*, *116*, 1044–1056.
Williams, M., and R. A. Houze (1987), Satellite-observed characteristics of winter monsoon cloud clusters, *Mon. Weather Rev.*, *115*, 505–519.
Willoughby, H. E., J. A. Clos, and M. G. Shoreibah (1982), Concentric eyewalls, secondary wind maxima, and the evolution of the hurricane vortex, *J. Atmos. Sci.*, *39*, 395–411.